Interleukin-18 Primes the Oxidative Burst of Neutrophils in Response to Formyl-Peptides: Role of Cytochrome b558 Translocation and N-Formyl Peptide Receptor Endocytosis

Carole Elbim,[1,2] Cécile Guichard,[1] Pham M. C. Dang,[1] Michèle Fay,[1] Eric Pedruzzi,[1]
Hélène Demur,[2] Cécile Pouzet,[3] Jamel El Benna,[1]
and Marie-Anne Gougerot-Pocidalo[1,2]*

Institut National de la Santé et de la Recherche Médicale, Unité 479,[1] and Institut National de la Santé et de la Recherche Médicale, IFR 02,[3] Faculté Xavier Bichat, and Service d'Immunologie et d'Hématologie, Centre Hospitalo-Universitaire Xavier Bichat,[2] Paris, France

Using flow cytometry, we observed that interleukin-18 (IL-18) primed human neutrophils (PMNs) in whole blood to produce superoxide anion ($O_2^{\circ-}$) in response to N-formyl peptide (fMLP) stimulation, whereas IL-18 alone had no significant effect. In contrast to tumor necrosis factor alpha (TNF-α), which is a cytokine known to strongly prime $O_2^{\circ-}$ production, IL-18 did not induce either $p47^{phox}$ phosphorylation or its translocation from the cytosol to the plasma membrane. However, IL-18 increased PMN degranulation, as shown by increased levels of cytochrome b558 and CD11b expression at the PMN surface. Moreover, addition of IL-18 to whole blood for 45 min reduced the ability of PMNs to bind to fMLP, suggesting endocytosis of fMLP receptors, as visualized by confocal microscopy. 2,3-Butanedione 2-monoxime, which inhibits endosomal recycling of plasma membrane components back to the cell surface, concomitantly accentuated the diminution of fMLP binding at the PMN surface and increased IL-18 priming of $O_2^{\circ-}$ production by PMNs in response to fMLP. This suggests that fMLP receptor endocytosis could account, at least in part, for the priming of $O_2^{\circ-}$ production. In addition, genistein, a tyrosine kinase inhibitor, and SB203580, a p38 mitogen-activated protein kinase (p38MAPK) inhibitor, completely reversed the decreased level of fMLP binding and increased the level of CD11b expression after IL-18 treatment. Flow cytometric analysis of intact PMNs in whole blood showed that IL-18 increased p38MAPK phosphorylation and tyrosine phosphorylation. In particular, IL-18 induced phosphorylation of focal adhesion kinase ($p125^{FAK}$), which has been implicated in cytoskeleton reorganization. Taken together, our findings suggest several mechanisms that are likely to regulate cytokine-induced priming of the oxidative burst in PMNs in their blood environment.

Polymorphonuclear neutrophils (PMNs) play a critical role in host defenses against invading microorganisms. In response to pathogens, PMNs move from the bloodstream into infected tissues, where their activation triggers the rapid production of reactive oxygen species (ROS), in what is known as the oxidative burst (1). The generation of microbicidal oxidants by neutrophils results from the activation of NADPH oxidase (4). This multicomponent enzyme system is inactive in resting cells, and its various components are distributed between the cytosol and membranes. The major membrane component, cytochrome b558, is composed of two subunits ($gp91^{phox}$ and $p22^{phox}$) and is located in specific or gelatinase granules and in the plasma membrane of resting neutrophils; the cytosolic components consist of four major proteins: $p47^{phox}$, $p67^{phox}$, $p40^{phox}$, and Rac 2, a small G protein (2). When PMNs are activated by stimuli such as N-formyl peptide derived from bacteria (fMLP) or phorbol myristate acetate, some of the cytosolic components become phosphorylated and migrate to the membrane, where they assemble as an active complex.

$p47^{phox}$ phosphorylation plays a critical role in the assembly and activation of the NADPH oxidase (9, 13).

PMNs can exist in three different activation states, namely, the resting, primed, and activated states. The priming process has been demonstrated in vitro by pretreating PMNs with a substimulatory concentration of a pharmacological agent, which subsequently enhances the PMN response to a second stimulus. In particular, priming of the PMN oxidative burst occurs in response to fMLP after pretreatment with a number of inflammatory mediators, including tumor necrosis factor α (TNF-α), granulocyte-macrophage colony-stimulating factor (GM-CSF), and bacterial lipopolysaccharide (LPS) (6, 8, 10, 15, 16). The mechanisms underlying the priming process are poorly understood, although some studies have suggested that priming with various agonists may be regulated at the receptor and the postreceptor levels. We (6, 10) and others (8) have shown that priming agents such as TNF-α, GM-CSF, and LPS induce partial $p47^{phox}$ phosphorylation in primed PMNs. However, other candidate priming mechanisms include increased levels of membrane expression of cytochrome b558 (8, 28, 44), increased levels of expression and cycling of triggering receptors such as fMLP receptors (fMLP-R) (19, 41), activation of heterotrimeric G proteins (29), as well as some other mechanisms (12, 22).

Interleukin-18 (IL-18) is a recently described member of the

---

* Corresponding author. Mailing address: Unité INSERM U479, Faculté de Médecine Xavier Bichat, 16 rue Henri Huchard, 75877 Paris Cedex 18, France. Phone: (33) 1 44 85 62 10. Fax: (33) 1 44 85 62 07. E-mail: pocidalo@bichat.inserm.fr.

IL-1 cytokine family (21, 35). Initially characterized by its capacity to promote Th1 responses in synergy with IL-12, IL-18 has been reported to modulate PMN functions and especially to prime the oxidative burst of isolated PMNs (25, 45). Isolation procedures may alter PMN responses, and study of the PMN responses in whole blood (when this is technically possible) therefore seems to be more suitable for unraveling how circulating PMNs in the resting state become activated. The effect of IL-18 on the PMN oxidative burst in whole blood has not previously been investigated, and the mechanisms of IL-18 priming were poorly understood.

Here we analyze the effects of IL-18 on the PMN oxidative burst in whole blood and the mechanisms of IL-18 priming by comparing them with those of TNF-α, the priming effect of which has been extensively studied. We first studied in whole blood the following major steps that lead to the activation of NADPH oxidase: (i) PMN degranulation by means of CD11b expression and cytochrome b558 translocation, (ii) fMLP binding at the PMN surface, and (iii) the participation of tyrosine kinases, especially p125^{FAK}, and mitogen-activated protein kinases (MAPKinases) in these processes. We also used isolated PMNs to study p47^{phox} phosphorylation, which we have previously shown to be a major event in TNF-α priming of the PMN oxidative burst (10).

MATERIALS AND METHODS

Reagents. The reagents used and their sources were as follows: human recombinant IL-18 (rhIL-18; 5 μg/ml; MBL, Tokyo, Japan); human recombinant TNF-α (rhTNF-α; 10^5 U/ml), and human recombinant IL-1β (rhIL-1β; 10^5 U/ml), R&D, Abington, United Kingdom; hydroethidine, Fluka, Buchs, Switzerland; fMLP (N-formyl-methionyl-leucyl-phenylalanine), fluorescein-conjugated formyl-Nle-Leu-Phe-Nle-Tyr-Lys, primaquine, 2,3-butanedione 2-monoxime (BDM), colchicine, diisopropylfluorophosphate, and a protease inhibitor mixture, Sigma Chemical Co., St. Louis, Mo.; SB203580, PD98059, U0126, genistein, wortmannin, and GF109203X, Calbiochem, La Jolla, Calif.; fluorescein-conjugated anti-human CD11b monoclonal antibody (MAb), Immunotech, Marseille, France; fluorescein-conjugated goat antimouse antibody, Nordic Immunology, Tilburg, The Netherlands; fluorescein-conjugated anti-human CD15 MAb, phycoerythrin-conjugated anti-human fMLP-R MAb, fluorescein-conjugated goat anti-rabbit immunoglobulin (Ig), mouse anti-human phosphotyrosine MAb, mouse antifocal adhesion kinase (p125^{FAK}) phosphospecific MAb, and mouse anti-p38MAPK and anti-ERK1/2 phosphospecific MAbs, Pharmingen, Becton Dickinson, San Jose, Calif.; rabbit anti-human p22^{phox} polyclonal antibody, Santa Cruz Biotechnology, Santa Cruz, Calif.; Dako LSAB alkaline phosphatase kit, Dakopatts, Glostrup, Denmark; [^{32}P]orthophosphoric acid, NEN Life Science Products; and rabbit polyclonal antibodies against p47^{phox}, anti-p22^{phox}, and anti-gp91^{phox}, generous gifts from B. M. Babior, Scripps Research Institute, La Jolla, Calif.

Neutrophil preparation. Human neutrophils were isolated under LPS-free conditions by means of dextran sedimentation and Ficoll-Hypaque centrifugation of freshly drawn blood, as described previously (6).

Incubation of whole blood and isolated PMNs with IL-18 and fMLPs. One-milliliter samples of fresh blood from healthy donors, collected on lithium heparinate (10 U/ml), or 4 × 10^5 isolated PMNs were incubated with either rhIL-18 (1 to 500 ng/ml) diluted in phosphate-buffered saline (PBS) or PBS alone at 37°C for various times (15 to 60 min). fMLP (10^{-6} M) was then added for 1 to 5 min at 37°C. The reaction was then stopped and red blood cells were lysed with a fluorescent-activated cell sorter (FACS) lysing solution (Becton Dickinson, Mountain View, Calif.). After the samples were washed once, the white blood cells were resuspended in 1% paraformaldehyde. In some experiments, the samples were pretreated with primaquine (250 μg/ml), BDM (0.1 to 15 mM), colchicine (5 to 100 μg/ml), or protein kinase inhibitors (SB203580, 10 μM; PD98059, 50 μM; U0126, 50 μM; GF109203X, 5 μM; wortmannin, 250 nM; genistein, 100 μM). The concentration-dependent effects of these inhibitors were previously tested in whole blood (10), and the concentrations are in the same range as those used with the isolated PMNs. PMN viability was not altered under

our priming conditions, as assessed in terms of propidium iodide exclusion measured by means of flow cytometry.

NADPH oxidase activity. NADPH oxidase activity was measured by using a flow cytometric assay derived from the hydroethidine oxidation technique for activated phagocytes described by Rothe and Valet (37). Fluorescent ethidium (E$^+$) emits light in the orange wavelengths when it is exposed to laser excitation at 488 nm. This technique, which has been correlated to the superoxide dismutase-inhibitable reduction of ferricytochrome c (37), allowed us to study ROS production by PMNs in their blood environment. Whole-blood samples (1 ml) were preincubated for 15 min with hydroethidine (1,500 ng/ml) at 37°C. The samples were then incubated first with IL-18 and then with fMLP (10^{-6} M). Red blood cells were lysed as described above. The fixed samples were kept on ice until they were subjected to flow cytometric analysis on the same day.

Superoxide anion (O$_2^-$) production was also tested by using a continuous spectrophotometric assay of ferricytochrome c reduction by isolated PMNs. The specificity of O$_2^{\circ-}$ production was assessed by determination of the level of superoxide dismutase inhibition, as described previously (6).

Study of CD11b and p22^{phox} expression at the PMN surface. Whole-blood samples were either kept on ice or incubated with rhIL-18, rhTNF-α (100 U/ml), or PBS for 45 min at 37°C. Samples (100 μl) were incubated at 4°C for 30 min with fluorescein isothiocyanate (FITC)-conjugated anti-human CD11b MAb and rabbit anti-p22^{phox} polyclonal antibody, followed by incubation with FITC–goat anti-rabbit Ig antibody. Red blood cells were lysed as described above.

Study of fMLP binding to the PMN surface. Whole-blood samples were either kept on ice or incubated with rhIL-18, rhTNF-α (100 U/ml), or PBS as described above. The samples (100 μl) were then incubated at 4°C for 1 h with FITC-conjugated formyl-Nle-Leu-Phe-Nle-Tyr-Lys (FITC-fMLP). Red cells were then lysed with FACS lysing solution.

Study of intracellular tyrosine phosphorylation and activation of focal adhesion kinase and MAPKinases (ERK1/2 and p38MAPK). After incubation of whole blood with rhIL-18 (500 ng/ml) or PBS for 45 min at 37°C, the white blood cells obtained after red blood cell lysis were fixed with 2% paraformaldehyde–PBS (10 min at 37°C) and permeabilized in 90% methanol (30 min on ice), as described previously (17). After the cells were washed once, they were stained with anti-phosphotyrosine MAb, anti-p125^{FAK} phosphospecific MAb, and anti-MAPKinase (p38MAPK and ERK1/2) phosphospecific MAbs for 1 h at room temperature; washed once; and then incubated for 30 min with FITC-goat antimouse antibody. After the cells were washed once more, they were resuspended in 1% paraformaldehyde–PBS.

Flow cytometry analysis. For flow cytometry analysis we used a Becton Dickinson FACScalibur (Immunocytometry Systems, San Jose, Calif.) flow cytometer equipped with a 15-mW, 488-nm argon laser. Forward scatter and side scatter were used to identify the granulocyte population and to gate out other cells and debris. The purity of the gated cells was assessed with FITC- or phycoerythrin-(PE)-conjugated anti-CD3, anti-CD45, anti-CD14, and anti-CD15 antibodies (Becton Dickinson). Ten thousand events were counted per sample, and the fluorescence pulses were amplified by 4-decade logarithmic amplifiers. The green fluorescence of FITC–anti-CD11b antibody, FITC-fMLP, and FITC-goat antimouse antibody was recorded from 515 to 545 nm; and the orange fluorescence of hydroethidine was recorded from 549 to 601 nm. All the results were obtained with a constant photomultiplier gain value. The data were analyzed with CELL QUEST software, and the mean fluorescence intensity was used to quantify the responses. Nonspecific binding was determined with cells incubated with the same concentration of an irrelevant antibody of the same isotype or with nonimmune serum.

^{32}P labeling of neutrophils and stimulation, fractionation, and immunoprecipitation of p47^{phox}. PMNs were incubated in phosphate-free buffer containing 0.5 mCi of [^{32}P]orthophosphoric acid/10^8 cells/ml for 60 min at 30°C, as reported previously (6). The PMNs were then treated with rhIL-18, rhTNF-α, or rhIL-1β, as described above, and stimulated with 10^{-7} M fMLP for an additional 2 min. The reaction was stopped by the addition of ice-cold buffer and centrifugation at 400 × g for 7 min at 4°C. The cells were lysed by resuspending them in lysis buffer, as described previously (6, 14). The lysate was centrifuged at 10,000 × g for 20 min at 4°C in a TL 100 ultracentrifuge (Beckman, Fullerton, Calif.). The cleared supernatant was incubated overnight with anti-p47^{phox} antibody (1/200). p47^{phox} was then immunoprecipitated with gamma-bind G-Sepharose beads (Pharmacia Biotech, Uppsala, Sweden) (6). The proteins were analyzed by sodium dodecyl sulfate-polyacrylamide gel electrophoresis (SDS-PAGE) on a 10% polyacrylamide gel and then blotted onto nitrocellulose membranes and detected by autoradiography.

Translocation of p67^{phox} and p47^{phox} from the cytosol to the PMN membrane. Suspensions of 25 × 10^6 PMNs/ml were incubated at 37°C with IL-18 or Hanks balanced salt solution with Ca^{2+}/Mg^{2+} for 45 min. The PMNs were then stim-

ulated with fMLP (10^{-7} M) for 3 min while the mixture was gently shaken. The cells were diluted in 4 volumes of ice-cold buffer and pelleted by centrifugation at $400 \times g$ for 8 min at 4°C. The pellets were resuspended in relaxation buffer containing 1 mM piperazine-N,N'-bis(2-ethanesulfonic acid) (pH 7.3), 10 mM KCl, 0.3 mM NaCl, 0.35 mM MgCl$_2$·6H$_2$O, 2 mM phenylmethylsulfonyl fluoride, 1.25 mM EGTA, 10 µg of leupeptin per ml, pepstatin, and aprotinin (6). The cells were disrupted by sonication (four times for 10 s each time) at 4°C, and the suspension was then centrifuged at $400 \times g$ for 8 min. The postnuclear supernatant was loaded onto a discontinuous sucrose gradient (50% sucrose, 15% sucrose), diluted in relaxation buffer, and centrifuged for 45 min at 200,000 $\times g$. The membrane fraction in the 15% sucrose layer was collected and washed once with relaxation buffer. Following SDS-PAGE on 10% acrylamide gels, the proteins were transferred to nitrocellulose filters. The filters were incubated for 1 h at room temperature in 50 mM Tris–150 mM NaCl–0.1% Tween 20 (TBST) containing 1% (wt/vol) fat-free dried milk. The nitrocellulose membranes were incubated for 1 h with specific rabbit antibodies against p47^{phox} and p67^{phox} at a 1/5,000 dilution. Following five washes with TBST, the membranes were incubated with a donkey antirabbit antibody conjugated to horseradish peroxidase. After five washes with TBST, revelation was performed by a chemiluminescence method (ECL; Amersham Life Sciences, Arlington Heights, Ill.), according to the instructions of the manufacturer.

Immunocytochemical staining of intracellular p22^{phox} and gp91^{phox}. Whole-blood samples were either kept on ice or incubated with rhIL-18 (500 ng/ml) for 45 min. Smears of unstimulated or stimulated blood samples were then air dried for 24 h and incubated in cold acetone-methanol (1:1) at 4°C for 10 min in order to fix and permeabilize the membranes (17). Nonspecific staining was blocked by incubation with the blocking reagent from the Dako LSAB alkaline phosphatase kit for 5 min. The smears were then incubated with a rabbit anti-human p22^{phox} antibody (0.8 µg/ml) or a rabbit anti-human gp91^{phox} antibody (0.8 µg/ml) for 10 min, followed by sequential incubation in 10-min steps with a biotinylated goat anti-rabbit and alkaline phosphatase-labeled streptavidin. Staining was revealed with a freshly prepared substrate-chromogen solution. Positive staining developed as a fuchsia-colored reaction product. The negative control consisted of smears incubated with nonimmune rabbit serum, and positive controls were incubated with an anti-CD11b MAb, followed by incubation with a biotinylated goat antimouse antibody.

Confocal laser scanning microscopy. Whole-blood samples were incubated at 4°C for 1 h with FITC–anti-human CD15 and PE–anti-human fMLP-R antibodies. After the samples were washed once with ice-cold PBS, they were incubated at 37°C with PBS or IL-18 (500 ng/ml) for 45 min. The red blood cells were lysed as described above, and the white blood cells were resuspended in 1% paraformaldehyde–PBS. The cells were then spun onto microscope slides at 500 rpm in a cytospin centrifuge (Shandon Southern Instruments) and mounted with an antiquenching reagent (Vectashield; Vector Laboratories, Burlingame, Calif.). The cells were examined by confocal laser scanning microscopy (LSM-510-META microscope; Zeiss, Oberkochen, Germany) equipped with a ×63 oil-immersion objective.

Statistical analysis. Data are presented as means ± standard error of the means (SEMs). Means were compared by the Mann-Whitney nonparametric comparison test. P values less than 0.05 were considered significant.

RESULTS

IL-18 primes the oxidative burst of whole-blood PMNs in response to fMLPs. IL-18 alone did not induce O$_2^{°-}$ production by PMNs in their blood environment (Fig. 1). However, preincubation of the whole blood with increasing concentrations of IL-18 from 0.1 to 500 ng/ml for 45 min, followed by exposure to 10^{-6} M fMLP for 5 min, increased the PMN oxidative burst in a concentration-dependent manner, reaching a maximum value at 500 ng/ml. This priming effect was approximately one-half that observed with the optimum concentration of TNF-α in whole blood (mean fluorescence intensities ± SEMs [$n = 10$], 108.7 ± 14.7 and 54.4 ± 5.6 for TNF-α and IL-18, respectively). Preincubation with cycloheximide (20 µg/ml), an inhibitor of protein synthesis, for 5 min before the addition of hydroethidine did not modify the priming effect of IL-18. When an anti-IL-18 MAb was added before incubation with IL-18 and fMLP, hydroethidine oxidation was suppressed.
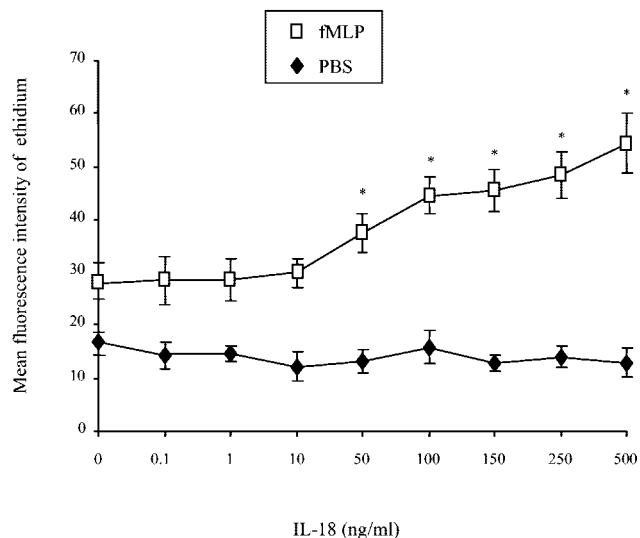

FIG. 1. Effect of IL-18 on the PMN oxidative burst in whole blood. After preincubation with hydroethidine (1,500 ng/ml) for 15 min at 37°C, whole blood was pretreated with PBS or various concentrations of IL-18 for 45 min, and then with PBS or fMLP (10^{-6} M) for 5 min. The mean fluorescence intensity of the ethidium (E$^+$) content was recorded as described in Materials and Methods. Values are expressed as means ± SEMs ($n = 10$). The mean fluorescence intensity of the sample preincubated with TNF-α (100 U/ml) and then stimulated with fMLP was 108.7 ± 14.7. ∗, significantly different from the results for the sample pretreated with PBS and then stimulated with fMLP ($P < 0.05$).

This finding rules out the possibility that the priming effect of IL-18 could be attributable to a contaminant such as an endotoxin. The priming effect of IL-18 on the PMN oxidative burst was also demonstrated by using the spectrophotometric assay of cytochrome c reduction on isolated PMNs in response to fMLP (10^{-7} M for 5 min) (data not shown).

A kinetic study showed that the mean fluorescence intensity of the ethidium content increased from 17.2 ± 1.1 after preincubation with IL-18 (500 ng/ml) for 15 min to a maximum of 56.5 ± 6.0 ($n = 3$) after 45 min (data not shown); we therefore used a preincubation time of 45 min throughout the rest of the study.

IL-18 does not induce phosphorylation or translocation of p47^{phox}. Phosphorylation of p47^{phox} has been implicated in the priming effect of GM-CSF and TNF-α on the PMN oxidative burst (6, 10). We therefore analyzed the effect of IL-18 on this process. As shown in Fig. 2, in keeping with previous data, p47^{phox} phosphorylation in TNF-treated neutrophils was clearly higher than that in untreated cells (10). In contrast, p47^{phox} phosphorylation was not increased in the PMNs treated with IL-18 or IL-1. Furthermore, kinetics analysis showed no phosphorylation of p47^{phox} at any time (10 to 45 min) (data not shown). As translocation of cytosol components to the membrane is a major step in the activation of NADPH oxidase, we also tested the effect of IL-18 on the translocation of p47^{phox} and p67^{phox}. As shown in Fig. 3, neither IL-18 nor TNF-α alone induced the translocation of p47^{phox} or p67^{phox} to the membrane; however, TNF-α significantly increased fMLP-induced p47^{phox} and p67^{phox} translocation (positive control), whereas IL-18 had no such effect.
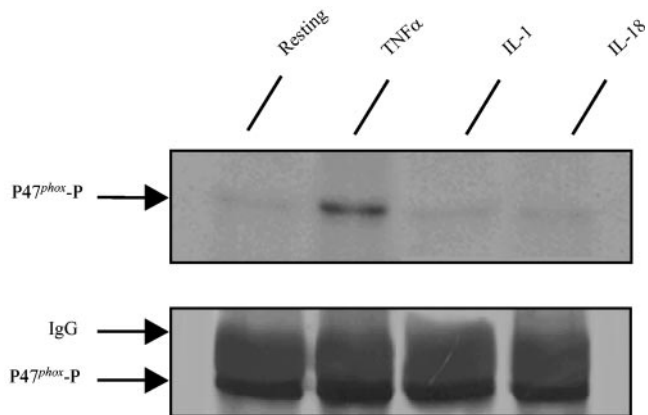
FIG. 2. Effects of IL-18, IL-1, and TNF-α on p47^{phox} phosphorylation. ^{32}P-labeled neutrophils were incubated with IL-18 (500 ng/ml), TNF-α (100 U/ml), or IL-1β (50 ng/ml) for 45 min. p47^{phox} was immunoprecipitated and analyzed by SDS-PAGE transfer and revealed by autoradiography ([^{32}P]p47^{phox}) with an anti-p47^{phox} antibody. Data are representative of those from three experiments.

IL-18-induced translocation of cytochrome b558 and CD11b to the plasma membrane. Unlike TNF-α, IL-18 did not induce phosphorylation of the cytosolic NADPH oxidase component p47^{phox}, suggesting that the priming effect on O$_2$$^{\circ-}$ production must involve some other mechanism. We therefore investigated the effect of IL-18 on the translocation of flavocytochrome b558 to the PMN surface by means of immunocytochemical staining after PMN permeabilization. Rabbit anti-human p22^{phox} antibody staining, revealed with a goat antirabbit antibody, was positive inside unstimulated PMNs, with no staining at the PMN surface; however, when immunostaining was performed with IL-18-stimulated PMNs, the staining was located at the PMN membrane (Fig. 4). No staining was observed with nonimmune rabbit serum. Similar results were obtained with anti-gp91^{phox} antibody (data not shown). Furthermore, using a rabbit anti-human p22^{phox} antibody, we confirmed the IL-18-induced increase in the level of expression of p22^{phox} at the cell surface (Fig. 5). This finding suggests that IL-18 primes NADPH oxidase by increasing the level of expression of cytochrome b558 derived from intracellular stores, such as specific granules, on the plasma membrane. In order to confirm these findings, we measured the level of expression of CD11b, another marker of specific granules. IL-18 also induced the translocation of CD11b to the PMN membrane: an increased level of CD11b expression was observed with an anti-CD11b antibody by the same immunochemistry technique and was confirmed by flow cytometry. This increase was shown to occur in an IL-18-concentration-dependent manner (Fig. 5).

In order to block this process and to analyze the effect on priming, we used colchicine, which inhibits neutrophil degranulation (32). Pretreatment of whole blood with increasing concentrations of colchicine inhibited the IL-18-induced increase in CD11b expression and its priming effect on O$_2$$^{\circ-}$ production in response to fMLP (Fig. 6).

Involvement of fMLP receptor internalization in IL-18 priming of the PMN oxidative burst. FMLP-Rs are also stored in specific or gelatinase granules, and modulation of their expression at the PMN surface could result from granule exocytosis and from a cycling process, which has also been impli-
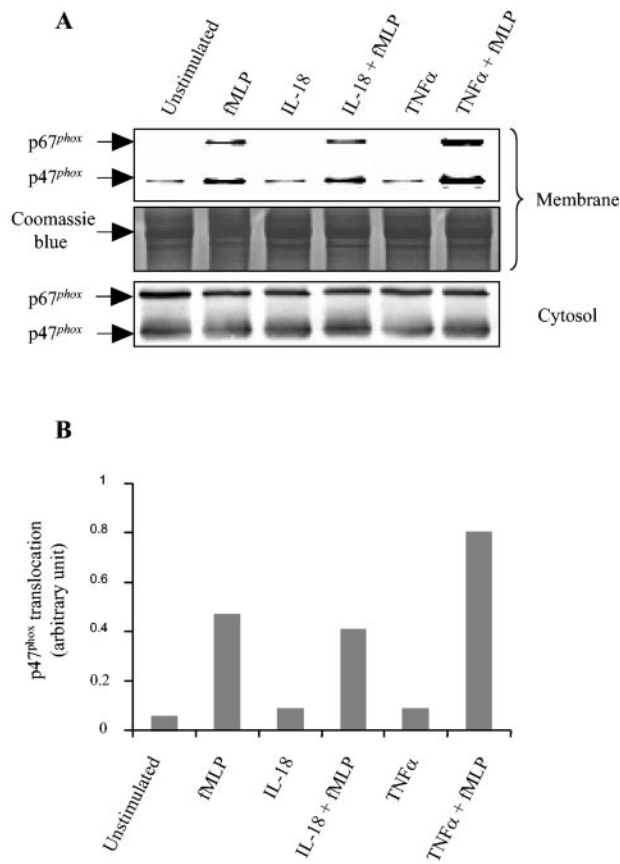

FIG. 3. Effects of IL-18 on p47^{phox} and p67^{phox} translocation to the PMN membrane. Isolated neutrophils were incubated with IL-18 (500 ng/ml) or buffer. Following stimulation with fMLP (10^{-7} M) for 1 min, PMN fractions were prepared as described in Materials and Methods. Acrylamide gels (10%) were loaded with 20 μg of protein, and then Western blotting (A) of membranes and the cytosol was performed with antibodies directed against p47^{phox} and p67^{phox}. Equal amounts of protein were loaded and checked by Coomassie blue staining. (B) Quantification of p47^{phox} translocation at the membrane, as determined by densitometry. The data are representative of those from three experiments.

cated in cytokine-induced priming of the oxidative burst (19, 41). We therefore analyzed the effect of IL-18 on the binding of FITC-fMLP at the PMN surface. These binding experiments were performed at 4°C to avoid the consequences of ligand-receptor interactions and to isolate the effect of IL-18 on fMLP-R expression.

As shown in Table 1, incubation of whole blood with IL-18 (50 and 500 ng/ml) for 45 min significantly decreased the fluorescence intensity of FITC-fMLP compared to that of samples incubated with PBS. Similar results were obtained with PE–anti-fMLP-R antibody; in fact, the mean fluorescence intensity of the sample incubated with IL-18 (500 ng/ml) (19.7 $\pm$ 2.5) was significantly lower than that of the sample incubated with PBS (28.5 $\pm$ 3.1). However, this decrease never matched the mean fluorescence intensity value obtained with the isotypic control (19.7 $\pm$ 2.5 and 5.0 $\pm$ 0.7, respectively), indicating that available fMLP-Rs always persisted at the cell surface after IL-18 stimulation. This reduction of the mean fluorescence intensity was also observed after shorter incubation
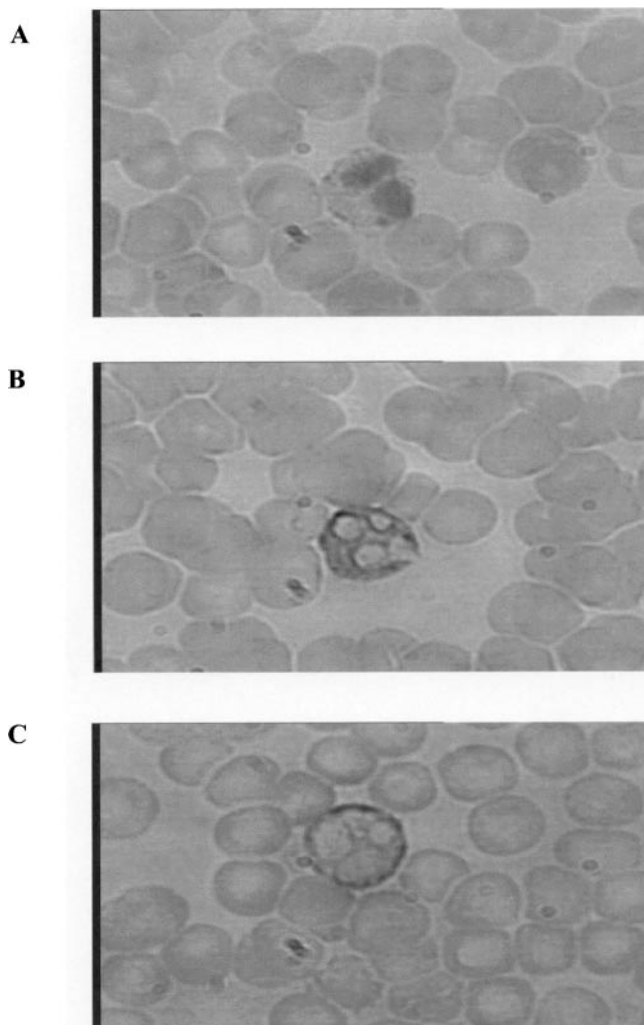
FIG. 4. Immunocytochemical staining of p22^{phox} in resting and IL-18-stimulated PMNs in whole-blood smears. (A) Negative control, which consisted of no staining with nonimmune rabbit serum followed by incubation with a biotinylated goat anti-rabbit and alkaline phosphatase-labeled streptavidin, as described in Materials and Methods; (B) intracellular fuchsia-colored staining was observed with the rabbit anti-human p22^{phox} polyclonal antibody (0.8 μg/ml), revealed as described for panel A; (C) fuchsia-colored staining at the PMN membrane was observed with the rabbit anti-human p22^{phox} polyclonal antibody (revealed as described for panel A) after IL-18 stimulation. Smears were examined by light microscopy. Magnifications, ×750.

FIG. 5. Effects of IL-18 on p22^{phox} and CD11b expression at the PMN surface. After preincubation with PBS (IL-18 at 0 ng/ml) or IL-18 (0.1 to 500 ng/ml) for 45 min, whole blood was incubated with anti-p22^{phox} and anti-CD11b antibodies at 4°C for 30 min. The mean fluorescence intensity was recorded as described in Materials and Methods. Values obtained with nonimmune rabbit serum or with an irrelevant antibody of the same isotype were subtracted. Values are expressed as means ± SEMs ($n = 4$). The mean fluorescence intensity of the sample incubated with TNF-α (100 U/ml) was 1,729 ± 89. *, significantly different from the results for the sample incubated with PBS ($P < 0.05$).

times (15 and 30 min) with IL-18 (500 ng/ml). No alteration of FITC-fMLP binding was observed from 1 to 5 min after IL-18 incubation. Under our experimental conditions, TNF-α (100 U/ml) also reduced the level of fMLP binding, and this effect was stronger and occurred more rapidly than that induced by IL-18 at its optimum priming concentration (500 ng/ml). This diminution of fMLP binding was reversed by preincubation of the sample with primaquine, an endocytosis inhibitor, whereas protease inhibitors had no effect, suggesting that IL-18 induced internalization of the fMLP-Rs (data not shown). This phenomenon was confirmed by confocal microscopy (Fig. 7). After being exposed to IL-18 for 45 min, fMLP-Rs were located deep
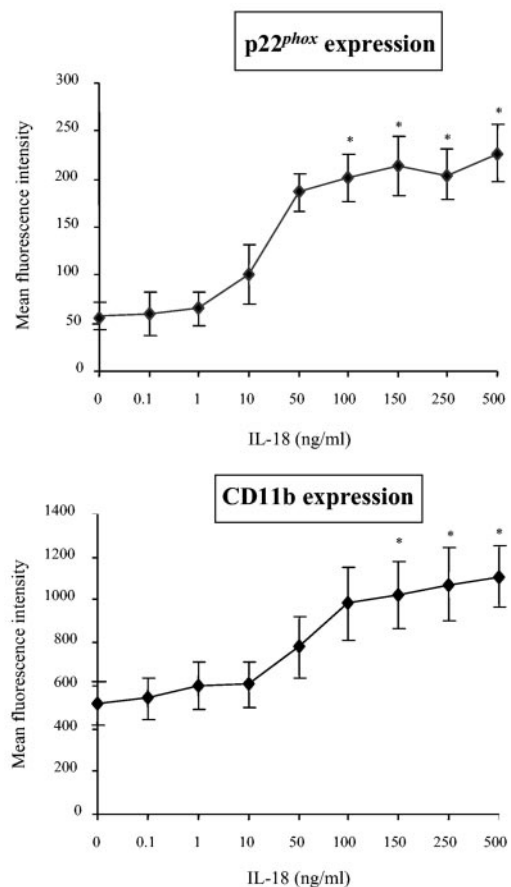
within the cell, whereas the CD15 antigen was located only on the surface of the cell.

In order to investigate the role of fMLP-R endocytosis in IL-18 priming, we analyzed the fMLP-induced PMN oxidative burst and fMLP binding after preincubation with BDM, an inhibitor of actomyosin ATPase, which has been reported to inhibit the recycling of plasma membrane components from endosomes back to the cell surface (33). We observed that 0.1 to 1 mM BDM potentiated the IL-18-induced decrease in fMLP binding at the PMN surface, suggesting fMLP-R accumulation in an intracytoplasmic compartment. Furthermore, BDM treatment also enhanced the priming effect of IL-18 on the oxidative burst in response to fMLP. These effects were reversed at higher concentrations (Table 2).

Signaling pathways involved in IL-18 effects. In order to investigate the signaling pathways involved in the effects of IL-18 on PMNs, we first analyzed the effects of kinase inhibitors on PMN degranulation and fMLP-R endocytosis. Myeloid
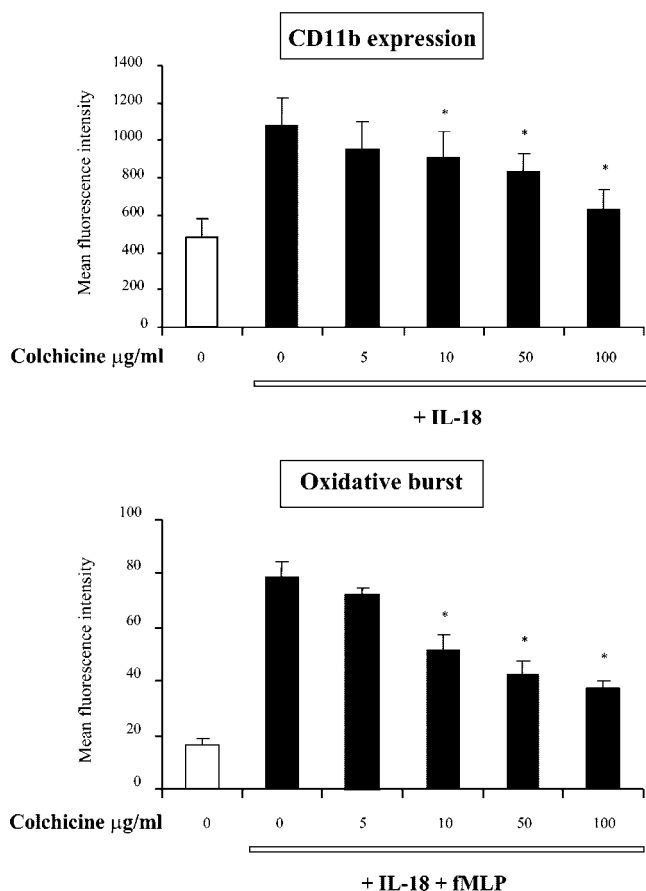
FIG. 6. Effects of colchicine on CD11b expression and the PMN oxidative burst after IL-18 priming. Samples were preincubated at 37°C with colchicine at various concentrations for 5 min before the addition of IL-18 (500 ng/ml) for 45 min. CD11b expression was measured with a mouse anti-human FITC–anti-CD11b antibody. The oxidative burst was measured by incubation of the samples with hydroethidine for 15 min before the addition of IL-18 and then stimulation with fMLP (10^{-6} M) for 5 min. The mean fluorescence intensity of the FITC–anti-CD11b antibody and the ethidium content were recorded as described in Materials and Methods. Values are expressed as means ± SEMs ($n = 3$). ∗, significantly different from the results for the samples without colchicine ($P < 0.05$).

cells, such as PMNs, are terminally differentiated short-lived cells that are resistant to transfection. An alternative strategy for studying the role of specific enzymes is to use cell-permeant pharmacological inhibitors.

As shown in Fig. 8, only genistein, a broad-specificity tyrosine kinase inhibitor, and SB203580, a p38MAPK inhibitor, completely reversed the IL-18-induced increase in the level CD11b expression and the IL-18-induced decrease in the level of fMLP binding. Genistein and SB203580 also completely reversed the IL-18-induced increase in the level of p22^{phox} expression (data not shown). In contrast, wortmannin (a PI3-kinase inhibitor), GF109203X (a protein kinase C inhibitor), and PD98059 and U0126 (MEK1/2 inhibitors) had no effect on IL-18-induced processes. Similar results were obtained after TNF-α stimulation. These findings suggest that IL-18 induces NADPH oxidase priming via tyrosine kinase- and p38MAPK-

TABLE 1. Effect of IL-18 on fMLP binding at the PMN surface[a]

Time (min)	Mean fluorescence intensity				
	PBS	TNF-α (100 U/ml)	IL-18		
			1 ng/ml	50 ng/ml	500 ng/ml
5	74 ± 4	76 ± 6	77 ± 5	75 ± 4	76 ± 6
10	71 ± 4	56 ± 5[b]	73 ± 7	71 ± 7	69 ± 1
15	69 ± 2	48 ± 1[b]	70 ± 4	64 ± 6	60 ± 5[b]
30	70 ± 7	46 ± 7[b]	65 ± 6	67 ± 5	55 ± 5[b]
45	59 ± 6	32 ± 4[b]	58 ± 6	53 ± 6[b]	41 ± 6[b]

[a] Whole blood was preincubated at 37°C for 5 to 45 min with PBS, TNF-α (100 U/ml), or IL-18 at various concentrations (1, 50, and 500 ng/ml), and then with FITC-fMLP (10^{-5} M) at 4°C for 30 min. The mean fluorescence intensity of FITC-fMLP was recorded as described in Materials and Methods. The mean fluorescence intensity of the sample preincubated at 4°C (resting PMN) was 77 ± 4. Values are expressed as means ± SEMs ($n = 4$).
[b] Significantly different from the results for the samples incubated with PBS.

dependent pathways, while PI3-kinase, protein kinase C, and ERK1/2 do not appear to be involved in this process.

To confirm the data obtained with the tyrosine kinase inhibitor, we studied the phosphotyrosine contents of intact cells by flow cytometry with a mouse anti-human phosphotyrosine MAb. As shown in Fig. 9, incubation of whole blood with IL-18 alone significantly increased the level of tyrosine phosphorylation after as little as 2 min compared to that for samples incubated with PBS.

Among the tyrosine kinases, focal adhesion kinase (p125^{FAK}) has been implicated in cytoskeleton reorganization, leading to G-protein-coupled receptor internalization (43) and granule release (39). We therefore tested the consequences of IL-18 pretreatment of PMNs on p125^{FAK} activation in whole blood. Incubation with IL-18 significantly increased the level of phosphorylation of p125^{FAK} compared to that obtained by incubation with PBS. The kinetics were similar to those observed with an antiphosphotyrosine antibody (Fig. 9).

In accordance with our data obtained with SB203580, a p38MAK inhibitor, we found that IL-18 significantly increased the level of p38MAPK phosphorylation (Fig. 9). This IL-18-induced increase reached a maximum after incubation for 15 min and therefore occurred later than p125^{FAK} phosphorylation. In contrast, and in keeping with the lack of an effect of the ERK1/2 inhibitor PD98059 (50 μM) on the effects of IL-18, IL-18 did not increase the level of ERK1/2 phosphorylation (data not shown).

Similar results were observed with TNF-α, although the effects of TNF-α on tyrosine, p125^{FAK}, and p38MAPK phosphorylation were significantly stronger than those of IL-18.

DISCUSSION

The findings from the present study show that IL-18 primes PMNs in their blood environment to produce $O_2^{\circ-}$ in response to fMLP. In contrast to TNF-α, IL-18 did not induce significant p47^{phox} phosphorylation, a critical mechanism in oxidative burst priming by TNF-α and GM-CSF (6, 10). However, IL-18 did induce PMN degranulation, as shown by increased levels of cytochrome b558 components (p22^{phox} and gp91^{phox}) and CD11b expression at the PMN surface. Incubation of whole blood with IL-18 for 45 min decreased the level of fMLP
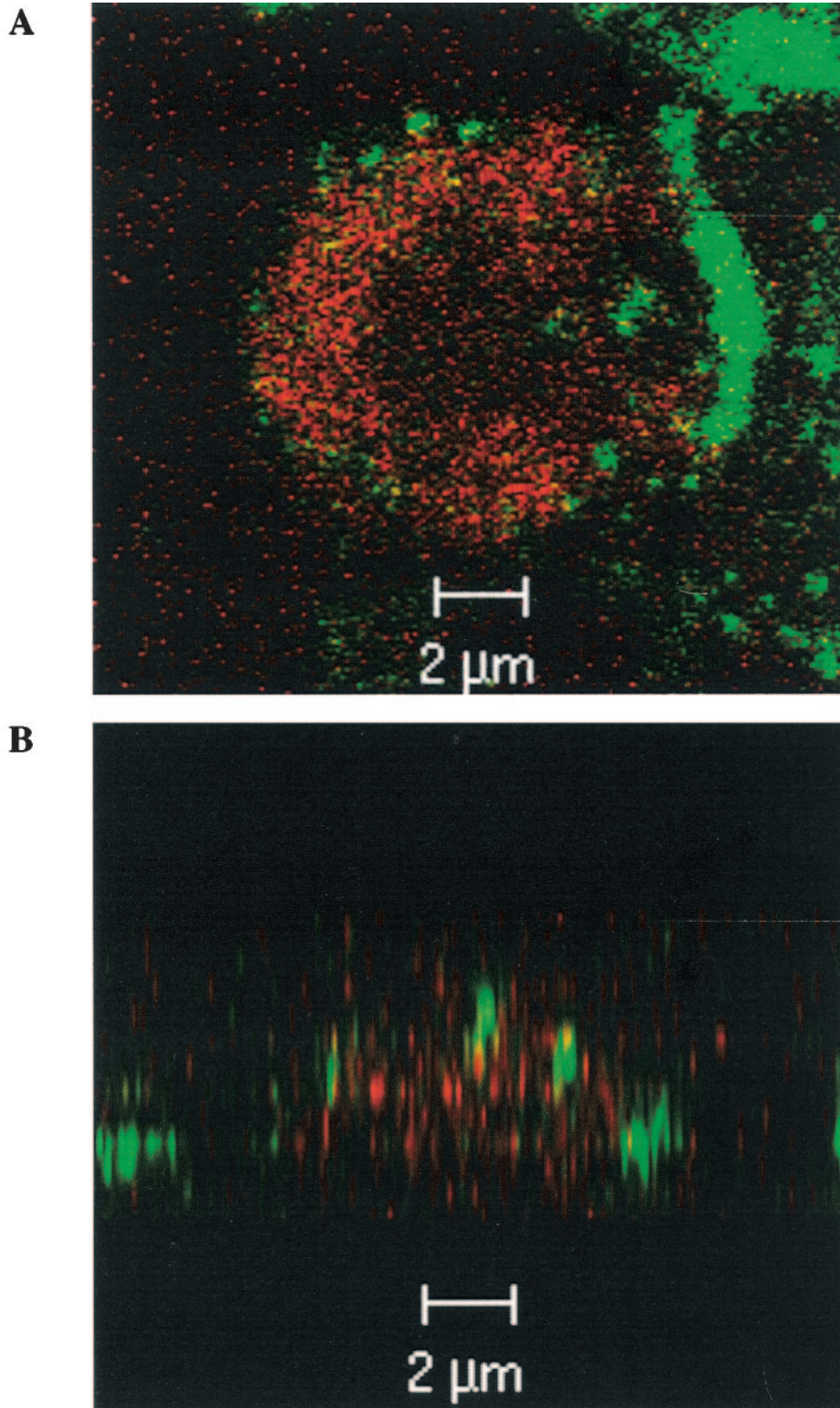
A

B

FIG. 7. Visualization of IL-18-induced fMLP-R endocytosis by confocal microscopy. Whole-blood samples were incubated at 4°C for 1 h with FITC–anti-human CD15 and PE–anti-human fMLP-R antibodies. After the samples were washed once in ice-cold PBS, they were incubated at 37°C with IL-18 (500 ng/ml) for 45 min. Images were obtained by confocal laser scanning microscopy. (A) Horizontal (*x-y*) section; (B) vertical (*x-z*) section. Thirty optical sections were used for three-dimensional reconstruction.

TABLE 2. Effects of BDM on PMN oxidative burst and fMLP binding after IL-18 activation

BDM concn (mM)	Mean fluorescence intensity of:			
	E^+ content[a]		FITC-fMLP[b]	
	PBS	IL-18 + fMLP	PBS	IL-18
0	15.8 ± 1.0	43.5 ± 5.6^c	58.3 ± 1.9	43.7 ± 1.3^c
0.1	13.0 ± 1.0	$59.0 \pm 1.0^{c,d}$	56.0 ± 1.5	$40.0 \pm 3.2^{c,d}$
1	15.0 ± 0.6	$67.3 \pm 6.2^{c,d}$	54.7 ± 1.7	$33.0 \pm 3.5^{c,d}$
5	15.5 ± 1.3	26.8 ± 3.5	55.7 ± 5.2	44.0 ± 5.7
10	15.5 ± 0.6	20.5 ± 3.1	55.0 ± 3.5	47.3 ± 4.9

[a] Samples were preincubated at 37°C with BDM at various concentrations for 5 min before the addition of hydroethidine for 15 min; the samples were then exposed to IL-18 (500 ng/ml) for 45 min and stimulated with fMLP (10^{-6} M) for 5 min. The mean fluorescence intensity of E^+ was recorded as described in Materials and Methods. Values are expressed as means $\pm$ SEMs ($n = 3$).

[b] Samples were preincubated for 20 min at 37°C with BDM at various concentrations and were then exposed to IL-18 (500 ng/ml) for 45 min. The mean fluorescence intensity of FITC-fMLP was recorded as described in Materials and Methods. Values are expressed as means $\pm$ SEMs ($n = 3$).

[c] Significantly different from the results for the samples incubated with PBS instead of IL-18.

[d] Significantly different from the results for the samples incubated with PBS instead of BDM.

binding at the PMN surface, suggesting that endocytosis of the fMLP-Rs may have occurred. In accordance with these findings, BDM, an inhibitor of recycling from endosomes to the cell surface, was shown to potentiate the reduction of fMLP binding induced by IL-18 and enhanced the IL-18 priming of the oxidative burst. Taken together, our data suggest several possible mechanisms that may be involved in cytokine-induced priming of the oxidative burst. In addition, we clearly demonstrated the involvement of p125^{FAK} phosphorylation and p38MAPK activation in the IL-18-priming effect of the oxidative burst in PMNs in their blood environment.

IL-18 alone did not directly activate the PMN oxidative burst. However, in accordance with previous data obtained with isolated PMNs (25, 45), IL-18 did prime PMNs in whole blood to produce $O_2^{\circ-}$ in response to fMLP. The kinetics that we observed in whole blood showed that maximum values were reached after 45 min. The fact that this response was slower than that reported by Wyman et al. (45) (45 versus 30 min) could be related to the fact that artifactual stimulation of the cells was minimized when isolation procedures were avoided.

IL-18 has recently been implicated in the pathogenesis of several inflammatory diseases (26) and severe sepsis (11, 18, 23). The mechanisms by which IL-18 promotes inflammatory responses may be related to its priming of the PMN oxidative burst. In addition, the ROS act as second messengers that lead to NF-κB activation in T cells and that initiate the expression of genes for Th1 cytokines (IL-2, TNF-α, and gamma interferon) (36). PMN activation by IL-18 may thus accentuate the role of IL-18 as a gamma interferon-inducing cytokine.

Priming of the PMN oxidative burst by various inflammatory agents could occur via different molecular mechanisms. In particular, partial phosphorylation of p47^{phox} at selective sites may facilitate the induction of p47^{phox} phosphorylation at other sites targeted by a secondary stimulus, such as fMLP, and thereby amplify the fMLP-induced translocation of p47^{phox} and p67^{phox} to the membrane. We clearly demonstrated that IL-18 did not induce phosphorylation of p47^{phox}, in keeping
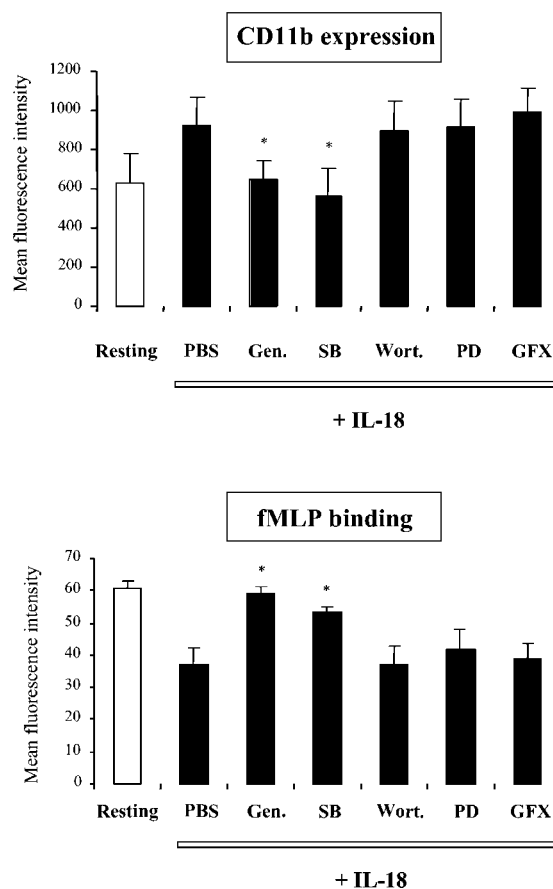

FIG. 8. Effects of kinase inhibitors on fMLP binding and CD11b expression after IL-18 activation. Samples were preincubated at 37°C with PBS or with various kinase inhibitors for 15 min at 37°C: genistein (Gen.) at 100 μM, SB203580 (SB) at 25 μM, wortmannin (Wort.) at 250 nM, PD98059 (PD) at 50 μM, or GF109203X (GFX) at 5 μM. Studies of CD11b expression and fMLP binding are described in the legend to Fig. 5 and in footnote a of Table 1, respectively. Values are expressed as means $\pm$ SEMs ($n = 3$). ∗, significantly different from the results for the sample pretreated with PBS and then incubated with IL-18.

with its lack of an effect on the translocation of p47^{phox} and p67^{phox} to the PMN membrane in response to fMLP. As expected, fMLP alone induced the translocation of p47^{phox} and p67^{phox} to the PMN membrane, and this translocation was potentiated by TNF-α. These data were obtained after PMN fractionation, with detection in each subcellular compartment. The difference in the techniques used may explain the discrepancies between our results and those reported by Wyman et al. (45), who observed IL-18-induced p47^{phox} translocation in whole cells by means of immunolabeling.

Mobilization of specific or gelatinase granules has been involved in the priming of NADPH oxidase. Indeed, exposure of PMNs to LPS (8), TNF-α (44), or granulocyte colony-stimulating factor (28) leads to increased flavocytochrome b expression at the plasma membrane. Our results extend these observations to another priming agent, IL-18, and provide further evidence that the translocation of gp91^{phox} and p22^{phox} is one mechanism by which PMN priming occurs. In addition, IL-18 increased the cell surface expression of CD11b, a marker of
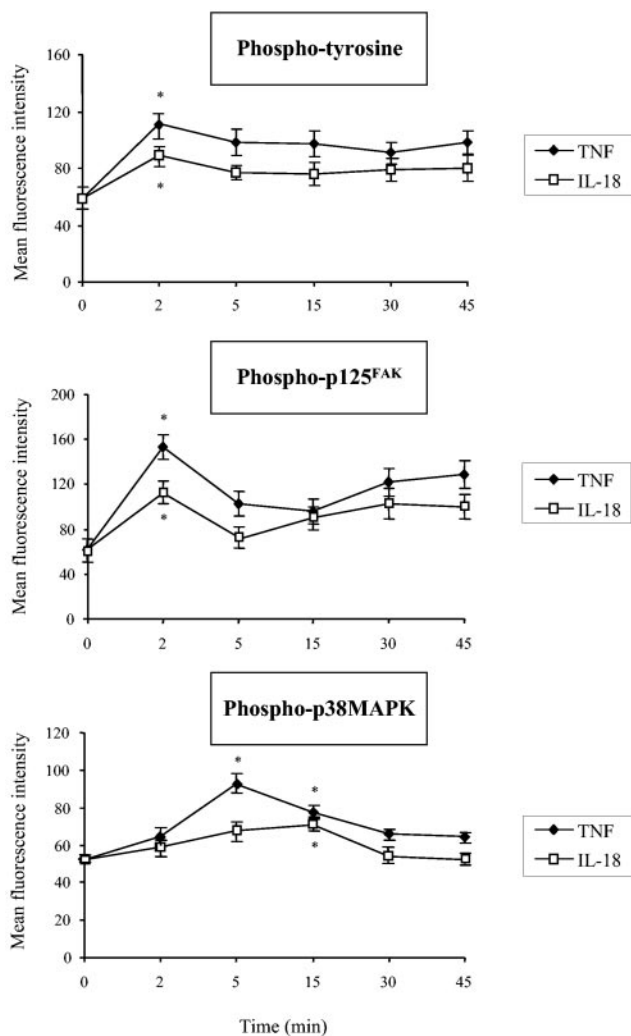
FIG. 9. Effects of IL-18 on intracellular tyrosine, p125^{FAK}, and p38MAPK phosphorylation. After preincubation of whole blood with PBS, IL-18 (500 ng/ml), or TNF-α (100 U/ml) for 2 to 45 min, the phosphotyrosine, phospho-p125^{FAK}, and phospho-p38MAPK contents were measured by flow cytometry with methanol-permeabilized cells, as described in Materials and Methods. Values obtained with an irrelevant antibody of the same isotype were subtracted. Values are expressed as means $\pm$ SEMs ($n = 3$). $*$, significantly different from the results for the sample incubated with PBS ($P < 0.05$).

specific and gelatinase granules, at the same time points and the same concentrations as those at which oxidative burst priming was observed. This IL-18-induced degranulation and the ROS production in response to fMLP were reversed by colchicine, an inhibitor of degranulation.

Evaluations of the modulation of fMLP-R expression and its association with the priming process have yielded contradictory data (19, 34, 41, 42). No increase in the level of FITC-fMLP binding was observed at any time during IL-18 incubation. In contrast, we observed that exposure of whole blood to IL-18 for 45 min significantly decreased the level of FITC-fMLP binding compared to that after exposure to PBS alone. This effect was not modified by preincubation of the samples with protease inhibitors, ruling out the possibility that the fMLP-Rs had been degraded by the action of proteases, which

could interfere with fMLP binding. In contrast, the decrease in fMLP binding induced by IL-18 was completely reversed by preincubating the samples with primaquine (250 μg/ml), an inhibitor of receptor endocytosis (7). Furthermore, after incubation of whole blood with IL-18 for 45 min, fMLP-R endocytosis was confirmed by confocal microscopy. As IL-18 triggered degranulation and also induced internalization of fMLP-Rs, which are also located in specific granules, a dynamic equilibrium between degranulation and fMLP-R endocytosis could be involved in the priming mechanisms induced by both IL-18 and TNF-α. Furthermore, endocytosis of the fMLP-R could be involved in its recycling back to the cell surface.

Previous studies have implicated fMLP-R endocytosis in desensitization phenomena (20). However, other studies have shown that fMLP-R internalization plays a key role in resensitization. A role of G-protein-coupled receptor endocytosis in cell signaling has also been reported (27). Our results, which demonstrated that BDM (1 mM) potentiated both an IL-18-induced decrease in the level of fMLP binding and IL-18 priming of the fMLP-induced oxidative burst, suggest a relationship between fMLP-R endocytosis and activation of ROS production by PMNs. The inhibition of the PMN oxidative burst observed at higher concentrations of BDM might have been related to disruption of PMN actin. Furthermore, BDM (1 mM) inhibited the IL-18-induced increased expression of CD11b and p22^{phox} at the cell surface. These results, in accordance with previously published data, suggest the possibility of a relationship between endocytosis and degranulation. In fact, Barlic et al. (3) demonstrated that the β-arrestin-mediated tyrosine kinase activation, receptor internalization, and the subsequent redistribution of β-arrestin–tyrosine kinase complexes to granules were required for chemokine-induced neutrophil granule exocytosis.

Tyrosine phosphorylation has been reported to play an important role in the signaling events leading to PMN degranulation (27, 31). Furthermore, tyrosine kinase activity is required for the internalization of receptors, with or without ligands, into clathrin-coated pits, which is one of the first steps in endocytosis and cycling of the receptors (24, 30). Our finding that genistein, a tyrosine kinase inhibitor with broad specificity, reduced the IL-18- and TNF-α-induced overexpression of CD11b and p22^{phox} at the PMN surface and also decreased the level of fMLP binding is in keeping with these data. Furthermore, our flow cytometric analysis of whole blood clearly demonstrated that in intact cells IL-18, like TNF-α, induced tyrosine phosphorylation; in particular, IL-18 and TNF-α increased the level of p125^{FAK} phosphorylation. p125^{FAK}, a member of a nonreceptor protein-tyrosine kinase family, has been implicated in ligand-independent endocytosis of membrane receptors (43) and in neutrophil degranulation processes in the presence of soluble fibrinogen, a factor present in whole blood (38).

The diminution of IL-18-induced CD11b expression that we observed after preincubating samples with SB203580 could be explained by the involvement of p38MAPK in neutrophil granule exocytosis after phosphorylation of these kinases by a mechanism involving an upstream tyrosine kinase (31). In addition, p125^{FAK} could control the activation of MAPKinases (5, 41). Using flow cytometric analysis of intact cells in whole

blood, we clearly observed that IL-18 induced p38MAPK phosphorylation and that this phosphorylation occurred later than p125^{FAK} phosphorylation. The lack of inhibition by the MEK1/2 inhibitors PD98059 and U0126 made it clear that different transduction pathways are involved, depending on the priming agent. Indeed, Suzuki et al. (40) clearly demonstrated that GM-CSF and TNF-α activated distinct MAPKinase subtype cascades in human neutrophils; GM-CSF preferentially activated ERK1/2, while TNF-α strongly activated p38MAPK.

Taken as a whole, these findings suggest that different cellular mechanisms may be involved in the cytokine-induced priming of the PMN oxidative burst. The most potent priming cytokines (TNF-α and GM-CSF) induce partial p47^{phox} phosphorylation that may facilitate further p47^{phox} phosphorylation and translocation to the membrane in response to a secondary stimulus. In contrast, less potent cytokines, such as IL-18, do not induce p47^{phox} phosphorylation. Similar results have been observed with granulocyte colony-stimulating factor and IL-1, which also have modest priming effects on the PMN oxidative burst in response to fMLP (10, 28). However, we found here that some of the mechanisms involved in their priming effects are shared by TNF-α and IL-18, which are representative of the cytokines with the most and least potent priming effects, respectively: TNF-α and IL-18 both induced degranulation of specific or gelatinase granules, enhancing the expression of their contents (especially of cytochrome b558) at the PMN surface and facilitating the formation of an active oxidase. Furthermore, both IL-18 and TNF-α induced endocytosis of G-protein-coupled receptors and could thereby induce cell signaling and regulate granule exocytosis. The latter mechanisms share a cascade of intracellular signals. The involvement of p38MAPK in IL-18 priming of the oxidative burst has been demonstrated in isolated PMNs. Using flow cytometry in whole blood, we clearly demonstrate here for the first time that focal adhesion kinase phosphorylation and p38MAPK activation are involved after IL-18 priming. Comparison of the effects of TNF-α and IL-18 at the transduction level showed that IL-18 had lower potency, which could possibly account, at least in part, for the differences between the functional effects of these two cytokines.

REFERENCES

1. **Babior, B. M.** 1984. Oxidants from phagocytes: agents of defense and destruction. Blood **64:**959–966.
2. **Babior, B. M.** 1999. NADPH oxidase: an update. Blood **93:**1464–1476.
3. **Barlic, J., J. D. Andrews, A. A. Kelvin, S. E. Bosinger, M. E. DeVries, L. Xu, T. Dobransky, R. D. Feldman, S. S. Ferguson, and D. J. Kelvin.** 2000. Regulation of tyrosine kinase activation and granule release through β-arrestin by CXCR1. Nat. Immunol. **87:**227–233.
4. **Chanock, S. J., J. El Benna, R. M. Smith, and B. M. Babior.** 1994. The respiratory burst oxidase. J. Biol. Chem. **269:**24519–24522.
5. **Coelho, A. L. J., M. S. De Freitas, A. Mariano-Oliveira, A. L. Oliveira-Carvalho, R. B. Zingali, and C. Barja-Fidalgo.** 2001. Interaction of disintegrins with human neutrophils induces cytoskeleton reorganization, focal adhesion kinase activation, and extracellular-regulated kinase-2 nuclear translocation, interfering with the chemotactic function. FASEB J. **15:**1643–1645.
6. **Dang, P. M., C. Dewas, M. Gaudry, M. Fay, E. Pedruzzi, M. A. Gougerot-Pocidalo, and J. El Benna.** 1999. Priming of human neutrophil respiratory burst by granulocyte/macrophage colony-stimulating factor (GM-CSF) involves partial phosphorylation of p47^{phox}. J. Biol. Chem. **274:**20704–20708.
7. **Davis, W., P. T. Harrison, M. J. Hutchinson, and J. M. Allen.** 1995. Two distinct regions of FcγRI initiate separate signalling pathways involved in endocytosis and phagocytosis. EMBO J. **14:**432–441.
8. **DeLeo, F. R., J. Renee, S. McCormack, M. Nakamura, M. Apicella, J. P. Weiss, and W. M. Nauseef.** 1998. Neutrophils exposed to bacterial lipopolysaccharide upregulate NADPH oxidase assembly. J. Clin. Investig. **101:**455–463.
9. **DeLeo, F. R., L. A. Allen, M. Apicella, and W. M. Nauseef.** 1999. NADPH oxidase activation and assembly during phagocytosis. J. Immunol. **163:**6732–6740.
10. **Dewas, C., P. M. Dang, M. A. Gougerot-Pocidalo, and J. El Benna.** 2003. TNF-α induces phosphorylation of p47^{phox} in human neutrophils: partial phosphorylation of p47^{phox} is common event of priming of human neutrophils by TNF-α and granulocyte-macrophage colony-stimulating factor. J. Immunol. **171:**4392–4398.
11. **Dinarello, C. A., and G. Fantuzzi.** 2003. Interleukin-18 and host defense against infection. J. Infect. Dis. **187**(Suppl. 2):S370–S384.
12. **Downey, G. P., T. Fukushima, L. Fialkow, and T. K. Waddell.** 1995. Intracellular signaling in neutrophil priming and activation. Semin. Cell. Biol. **6:**345–356.
13. **El Benna, J., L. P. Faust, and B. M. Babior.** 1994. The phosphorylation of the respiratory burst oxidase component p47phox during neutrophil activation: phosphorylation of sites recognized by protein kinase C and by proline-directed kinases. J. Biol. Chem. **269:**23431–23436.
14. **El Benna, J., L. P. Faust, J. L. Johnson, and B. M. Babior.** 1996. Phosphorylation of the respiratory burst oxidase subunit p47phox as determined by two-dimensional phosphopeptide mapping: phosphorylation by protein kinase C, protein kinase A, and a mitogen-activated protein kinase. J. Biol. Chem. **271:**6374–6378.
15. **Elbim, C., S. Chollet-Martin, S. Bailly, J. Hakim, and M. A. Gougerot-Pocidalo.** 1993. Priming of polymorphonuclear neutrophils by tumor necrosis factor α in whole blood: identification of two polymorphonuclear neutrophil subpopulations in response to formyl-peptides. Blood **82:**633–640.
16. **Elbim, C., S. Bailly, S. Chollet-Martin, J. Hakim, and M. A. Gougerot-Pocidalo.** 1994. Differential priming effects of proinflammatory cytokines on human neutrophil oxidative burst in response to bacterial N-formyl peptides. Infect. Immun. **62:**2195–2201.
17. **Elbim, C., H. Reglier, M. Fay, C. Delarche, V. Andrieu, J. El Benna, and M. A. Gougerot-Pocidalo.** 2001. Intracellular pool of IL-10 receptors in specific granules of human neutrophils: differential mobilization by proinflammatory mediators. J. Immunol. **166:**5201–5207.
18. **Emmanuilidis, K., H. Weighardt, E. Matevossian, C. D. Heidecke, K. Ulm, H. Bartels, J. R. Siewert, and B. Holzmann.** 2002. Differential regulation of systemic IL-18 and IL-12 release during postoperative sepsis: high serum IL-18 as an early predictive indicator of lethal outcome. Shock **18:**301–305.
19. **English, D., H. E. Broxmeyer, T. G. Gabig, L. P. Akard, D. E. Williams, and R. Hoffman.** 1988. Temporal adaptation of neutrophil oxidative responsiveness to N-formyl-methionyl-leucyl-phenylalanine. Acceleration by granulocyte-macrophage colony stimulating factor. J. Immunol. **141:**2400–2406.
20. **Ferguson, S. S.** 2001. Evolving concepts in G protein-coupled receptor endocytosis: the role in receptor desensitization and signaling. Pharmacol. Rev. **53:**1–24.
21. **Gu, Y., K. Kuida, H. Tsutsui, G. Ku, K. Hsiao, M. A. Fleming, N. Hayashi, K. Higashino, H. Okamura, K. Nakanishi, M. Kurimoto, T. Tanimoto, R. A. Flavell, V. Sato, M. W. Harding, D. J. Livingston, and M. S. Su.** 1997. Activation of interferon-γ inducing factor mediated by interleukin-1β converting enzyme. Science **275:**206–209.
22. **Hallett, M. B., and D. L. Lloyds.** 1995. Neutrophil priming: the cellular signals that say amber but not green. Immunol. Today **16:**264–268.
23. **Ikuta, S., S. Ono, M. Kinoshita, H. Tsujimoto, A. Yamauchi, and H. Mochizuki.** 2003. Interleukin-18 concentration in the peritoneal fluid correlates with the severity of peritonitis. Am. J. Surg. **185:**550–555.
24. **Kirchhausen, T., J. S. Bonifacino, and H. Riezman.** 1997. Linking cargo to vesicle formation: receptor tail interactions with coat proteins. Curr. Opin. Cell Biol. **9:**488–495.
25. **Leung, B. P., S. Culshaw, J. A. Gracie, D. Hunter, C. A. Canetti, C. Campbell, F. Cunha, F. Y. Liew, and I. B. McInnes.** 2001. A role of IL-18 in neutrophil activation. J. Immunol. **167:**2879–2886.
26. **Liew, F. Y., X. Q. Wei, and I. B. McInnes.** 2003. Role of interleukin 18 in rheumatoid arthritis. Ann. Rheum. Dis. **62**(Suppl. 2):ii, 48–50.
27. **Luttrell, L. M., and R. J. Lefkowitz.** 2002. The role of β-arrestins in the termination and transduction of G-protein-coupled receptor signals. J. Cell Sci. **115:**455–465.
28. **Mansfield, P. J., V. Hinkovska-Galcheva, J. A. Shayman, and L. A. Boxer.** 2002. Granulocyte colony-stimulating factor primes NADPH oxidase in neutrophils through translocation of cytochrome b558 by gelatinase-granule release. J. Lab. Clin. Med. **140:**9–16.
29. **McColl, S., D. Beauseigle, C. Gilbert, and P. H. Naccache.** 1990. Priming of the human neutrophil respiratory burst by granulocyte-macrophage colony-stimulating factor and tumor necrosis factor α involves regulation at a postcell surface receptor level. J. Immunol. **145:**3047–3053.

30. **Mellman, I.** 1996. Endocytosis and molecular sorting. Annu. Rev. Cell Dev. Biol. **12:**575–625.

31. **Mócsai, A., Z. Jakus, T. Vántus, G. Berton, C. A. Lowell, and E. Ligeti.** 2000. Kinase pathways in chemoattractant-induced degranulation of neutrophils: the role of p38 mitogen-activated protein kinase activated by Src family kinases. J. Immunol. **164:**4321–4331.

32. **Mollinedo, F., J. M. Nieto, and J. M. Andreu.** 1989. Cytoplasmic microtubules in human neutrophil degranulation: reversible inhibition by the colchicine analogue 2-methoxy-5-(2′,3′,4′-trimthoxyphenyl)-2,4,6-cycloheptatrien-1-one. Mol. Pharmacol. **36:**547–555.

33. **Neuhaus, E. M., and T. Soldati.** 2000. A myosin I is involved in membrane recycling from early endosomes. J. Cell Biol. **150:**1013–1026.

34. **O'Flaherty, J. T., A. G. Rossi, J. F. Redman, and D. P. Jacobson.** 1991. Tumor necrosis factor-α regulates expression of receptors for formyl-methionyl-leucyl-phenylalanine, leukotriene B4, and platelet-activating factor. Dissociation from priming in human polymorphonuclear neutrophils. J. Immunol. **147:**3842–3847.

35. **Okamura, H., H. Tsutsui, T. Komatsu, M. Yutsudo, A. Hakura, T. Tanimoto, K. Torigoe, T. Okura, Y. Nukada, K. Hattori, K. Akita, M. Namba, F. Tanabe, K. Konishi, S. Fukuda, and M. Kurimoto.** 1995. Cloning a new cytokine that induces IFN-γ production by T cells. Nature **378:**88–91.

36. **Pahl, H. L.** 1999. Activators and target genes of Rel/NF-κB transcription factors. Oncogene **18:**6853–6866.

37. **Rothe, G., and G. Valet.** 1990. Flow cytometric analysis of respiratory burst activity in phagocytes with hydroethidine and 2′,7′-dichlorofluorescin. J. Leukoc. Biol. **47:**440–448.

38. **Rubel, C., G. C. Fernandez, F. Alves Rosa, S. Gomez, M. B. Bompadre, O. A. Coso, M. A. Isturiz, and M. S. Palermo.** 2002. Soluble fibrinogen modulates neutrophil functionality through the activation of an extracellular signal-regulated kinase-dependent pathway. J. Immunol. **168:**3527–3535.

39. **Schlaepfer, D. D., S. K. Hanks, T. Hunter, and P. Van der Geer.** 1994. Integrin-mediated signal transduction linked to Ras pathway by GRB2 binding to focal adhesion kinase. Nature **372:**786–791.

40. **Suzuki, K., M. Hino, F. Hato, N. Tarsumi, and S. Kitagawa.** 1999. Cytokine-specific activation of distinct mitogen-activated protein kinase subtype cascades in human neutrophils stimulated by granulocyte colony-stimulating factor, granulocyte-macrophage colony-stimulating factor, and tumor necrosis factor-α. Blood **93:**341–349.

41. **Tennenberg, S. D., and J. S. Solomkin.** 1990. Activation of neutrophils by cachectin/tumor necrosis factor: priming of N-formyl-methionyl-leucyl-phenylalanine-induced oxidative responsiveness via receptor mobilization without degranulation. J. Leukoc. Biol. **47:**217–223.

42. **Tennenberg, S. D., D. E. Fey, and M. J. Lieser.** 1993. Oxidative priming of neutrophils by interferon-gamma. J. Leukoc. Biol. **53:**301–308.

43. **Wang, J., E. Guan, G. Roderiquez, V. Calvert, R. Alvarez, and M. A. Norcross.** 2001. Role of tyrosine phosphorylation in ligand-independent sequestration of CXCR4 in human primary monocytes-macrophages. J. Biol. Chem. **276:**49236–49243.

44. **Ward, R. A., M. Nakamura, and K. R. McLeish.** 2000. Priming of the neutrophil respiratory burst involves p38 mitogen-activated protein kinase-dependent exocytosis of flavocytochrome b558-containing granules. J. Biol. Chem. **24:**36713–36719.

45. **Wyman, T. H., C. A. Dinarello, A. Banerjee, F. Gamboni-Robertson, A. A. Hiester, K. M. England, M. Kelher, and C. C. Silliman.** 2002. Physiological levels of interleukin-18 stimulate multiple neutrophil functions through p38 MAP kinase activation. J. Leukoc. Biol. **72:**401–409.